Tri-*s*-triazine and Its Nitrogen Isoelectronic Equivalents: An ab Initio Study

Wenxu Zheng,[†] Ning-Bew Wong,*[,‡] Wai-Kee Li,*[,§] and Anmin Tian[†]

Faculty of Chemistry, Sichuan University, Chengdu, Sichuan 610064, People's Republic of China, and Department of Biology and Chemistry, City University of Hong Kong, Kowloon, and Department of Chemistry, The Chinese University of Hong Kong, Shatin, New Territories, Hong Kong

Received: July 13, 2004; In Final Form: October 18, 2004

To find the application of tri-*s*-triazine-based compounds, the geometric structures, electronic topologies, heats of formation, and relative specific impulses of tri-*s*-triazine and its nitrogen isoelectronic equivalents and decomposition of C_3N_{10} have been studied by quantum chemical methods. The results reveal that all these species have a rigid planar structure and a conjugation system over the tricyclic ring, which is beneficial to their stabilities. The molecular electrostatic potential analysis for all the species shows that the central region of the ring has a very strong positive electrostatic potential, which suggests that these heterocyclic rings should be applicable as an anion recognition module in cyclophane chemistry. Along with the replacement of the CH groups by nitrogen atoms in the tri-*s*-triazine molecule, the heats of formation and relative specific impulses for the substituted products increase substantially. This result suggests the equivalent **c** is a good candidate for high-energy-density material.

Introduction

The formation of molecular complexes (e.g., di-, tri-, oligo-, and polymers) is a conceivable way to increase density and stability and to improve the material properties of compounds.[1] The *s*-triazine monocyclic systems have been subjected to theoretical and experimental studies for a long time,[2] and they are known as an important set of conjugated heterocycles whose electronic properties are expected to show subtle differences from those of benzene due to the alternate replacement of CH groups by nitrogen atoms. These *s*-triazine-based chemicals are found to have various applications in the manufacturing of polymers, dyes, explosives, pesticides, and commodity chemicals.[3] But the tri-*s*-triazine-based molecules, composed of three fused *s*-triazine rings, received little attention. However, as macrocyclic heterosubstituted conjugated systems, these molecules probably have extraordinary properties. This has prompted us to investigate them systematically. In fact, the study of these molecules can be traced back to the 1830s.[4,5] At that time, a group of related nitrogen compounds, such as melem, hydromelonic acid, cyameluric chloride, cyameluric acid, etc., were known for their high heat stability, low solubility, and little chemical reactivity. However, because of their insolubility and chemical inertness, these compounds remained structural puzzles for more than a century. It was in 1937 that Pauling and Sturdivant first suggested a formulation for their common nucleus, a coplanar arrangement of three fused *s*-triazine rings.[6] Pauling apparently maintained an interest in tri-*s*-triazine, for reasons unknown, as the molecular formula of 2-azido-5,8-dihydroxytri-*s*-triazine was preserved on his office chalkboard at the time of his death in 1994.[7] However, in the past few decades, only the tri-*s*-triazine molecule itself was studied in detail.[8−11] Its structural and spectroscopic properties including an X-ray crystal structure analysis were studied. In addition, UV photoelectron spectra were taken and ab initio calculations were performed to explain the low basicity and the high stability.[8−11] In 2002, Kroke et al. synthesized 2,5,8-trichlorotri-*s*-triazine and found it was a promising starting material for numerous compounds including graphitic C_3N_4 phases.[12] In 2003, Schnick and co-worker determined the crystal structure of 2,5,8-triaminotri-*s*-triazine,[13] and in 2004, Gillan et al. reported the synthesis and crystal structure of 2,5,8-triazidotri-*s*-triazine.[14] To our knowledge, other derivatives of tri-*s*-triazine were only briefly mentioned in communications or patents and have not been characterized at all.[15] In our previous work, we have investigated many derivatives of tri-*s*-triazine in detail using ab initio methods.[16] In this paper we discuss the nitrogen isoelectronic equivalents of tri-*s*-triazine obtained from successive replacement of CH groups by nitrogen atoms.

Methods

The structures of the species under investigation were determined by analytic gradient techniques using the second-order Møller−Plesset perturbation (MP2) theory. Pople's standard 6-31G(d) basis set was used in conjunction with this method. The four structures were all confirmed as true local minima on the potential energy surface by the presence of only real frequencies after the corresponding vibrational analysis. Natural bond orbital (NBO) analysis[17−20] was performed at the MP2/6-31G(d) level on the basis of the optimized geometries. All these calculations were carried out using the Gaussian 98 program.[21]

The topological properties of the electronic charge density were characterized using the atoms in molecules (AIM) theory of Bader[22] with the AIM 2000 program package.[23] The AIM approach provides a rigorous procedure based upon the topology of $\rho(r)$ to partition the molecule into atomic fragments Ω bound by a zero flux surface for the gradient vector field of $\rho(r)$. A crucial element of the theory is the set of properties of the critical points in $\rho(r)$, where $\nabla\rho$ vanishes. The points lying between

* To whom correspondence should be addressed. E-mail: bhnbwong@cityu.edu.hk (N.-B.W.); wkli@cuhk.edu.hk (W.-K.L.).
[†] Sichuan University.
[‡] City University of Hong Kong.
[§] The Chinese University of Hong Kong.

10.1021/jp046909b CCC: $27.50
Published on Web 12/07/2004

bonded atoms are called bond critical points (BCPs), and whenever a set of bonded atoms forms a cycle, there also appear ring critical points (RCPs) with different topology features. Thus, whereas the BCP is a minimum of $\rho(r)$ along the bond path and a maximum in the interatomic surface, the RCP is a maximum on the ring line and a minimum in a locally perpendicular plane. Local properties at BCPs and RCPs convey valuable information about the molecular structure. The particular interest in this regard is the Laplacian of the density $\nabla^2\rho(r)$. In general, the Laplacian of a function measures to what extent this function is locally concentrated or depleted. When $\nabla^2\rho(r) < 0$ at a point, the electron density is locally concentrated (i.e., it is higher than at any of its neighboring points), and conversely, when $\nabla^2\rho(r) > 0$ at a point, $\rho(r)$ is locally depleted.

Molecular electrostatic potentials (MEPs)[24−26] of all the structures were calculated with Gaussian 98 at the MP2/6-31G(d) level at the optimized geometries shown in Figure 1 and plotted using gOpenMol 2.32[27,28] (Figure 5).

In the conventional ab initio calculations, the energies were determined at the G3(MP2) level.[29] At this level of theory, geometry optimization was carried out at the MP2(Full)/6-31G(d) level. To determine the energy E_e of a structure, single-point calculations at the levels of QCISD(T)/6-31G(d) and MP2(Full)/G3MP2large were carried out. In addition, higher level correction (HLC) was applied in the calculation of E_e. The HF/6-31G(d) frequency analysis was applied for the zero-point vibrational energy (ZPVE) correction at 0 K ($E_0 = E_e +$ ZPVE).

Upon obtaining the G3(MP2) energy of a species, its standard heat of formation $\Delta_f H$ at 298 K was calculated. Table 4 lists the total energies at 0 K (E_0) and enthalpies at 298 K (H_{298}) for the tri-*s*-triazine and its nitrogen isoelectronic equivalents calculated at the G3(MP2) level. To convert these results into $\Delta_f H$ values using the so-called atomization scheme,[30] the experimental[31] $\Delta_f H_0$ values of C (711.3 kJ mol^{-1}), H (216.0 kJ mol^{-1}), and N (470.8 kJ mol^{-1}), as well as the experimental $\Delta_f H_{298}$ values of C (716.7 kJ mol^{-1}), H (218.0 kJ mol^{-1}), and N (472.7 kJ mol^{-1}), are required.

Furthermore, on the basis of the heat of formation, we evaluated the high-energy-density material (HEDM) performance of these species using the relative specific impulse values introduced by Politzer et al.[32] We have described this method in detail in our previous work.[16]

Discussion

1. Geometries. After successive replacement of CH groups by nitrogen atoms in tri-*s*-triazine, three isoelectronic equivalents could be obtained. The local minima of these species were located at the MP2/6-31G(d) level, and the optimized geometries are depicted in Figure 1.

Hosmane et al. have determined the geometrical structure of tri-*s*-triazine.[33] Compared with their experimental results, our optimized structural parameters show a good agreement (see Figure 1). So the computational methods we selected in this study are reliable. As shown in Figure 1, all these optimized structures of tri-*s*-triazine and its three isoelectronic equivalents, **a**, **b**, and **c**, have a rigid planar geometry with D_{3h}, C_{2v}, C_{2v}, and D_{3h} symmetry, respectively. Examining the structural parameters involving heavy atoms summarized in Figure 1, we can find, for **a**, **b**, and tri-*s*-triazine, the N−N bond lengths are about 1.33 Å, the peripheral C−N bond lengths are about 1.34−1.35 Å, and the central C−N_{9b} bond lengths are about 1.37−1.40 Å. It should be noted that, after the replacement of CH groups by nitrogen atoms, the bond lengths for C−N bonds adjacent to the N−N bonds increase slightly while other C−N bond lengths almost do not change when compared with the corresponding C−N bond lengths in tri-*s*-triazine. At our computational level of theory, the equivalent **c** has a special structure: In the periphery of its tricyclic ring, there exist remarkable bond length differences between the adjacent N−N bonds (around 0.07 Å) and between the adjacent C−N bonds (about 0.06 Å). If there are no such differences, the structure is unstable (an imaginary frequency appears). However, for all the species, the replacement of CH groups by nitrogen atoms brings all bond angles close to 120°.

TABLE 1: Wiberg Bond Indices of the Bonds in the Ring for Tri-*s*-triazine and Its Nitrogen Isoelectronic Equivalents

	tri-*s*-triazine	a	b	c
$N_1-C_2(N_2)$	1.38	1.45	1.46	1.63
$C_2(N_2)-N_3$	1.38	1.45	1.44	1.28
$N_4-C_5(N_5)$	1.38	1.37	1.45	1.63
$C_5(N_5)-N_6$	1.38	1.38	1.46	1.28
$N_7-C_8(N_8)$	1.38	1.38	1.37	1.63
$C_8(N_8)-N_9$	1.38	1.37	1.37	1.28
N_1-C_{9a}	1.33	1.30	1.30	1.20
N_3-C_{3a}	1.33	1.30	1.32	1.46
N_9-C_{9a}	1.33	1.35	1.36	1.46
N_4-C_{3a}	1.33	1.35	1.31	1.20
N_6-C_{6a}	1.33	1.34	1.30	1.46
N_7-C_{6a}	1.33	1.34	1.36	1.20
$C_{3a}-N_{9b}$	1.03	1.05	1.06	1.04
$C_{6a}-N_{9b}$	1.03	1.02	1.04	1.04
$C_{9a}-N_{9b}$	1.03	1.05	1.04	1.04

2. Conjugation. From the geometric parameters, we can find that all the tricyclic systems have a uniform peripheral bond length, which ranges only from 1.33 to 1.38 Å. Moreover, the C−N bond lengths are shorter than that, 1.470 Å, of a normal C−N single bond and longer than that, 1.280 Å, of a normal C═N double bond. Also, the N−N bond lengths are between that, 1.45 Å, of a normal N−N single bond and that, 1.25 Å, of a normal N═N double bond. So there seems to be a delocalized system over each of these tricyclic species. Judging from the NBO analysis, the Wiberg bond indexes (WBIs)[18] (see Table 1) of peripheral N−C and N−N bonds are 1.20−1.63. Clearly, these data are between the standard WBIs values of the single bond (1.0) and the double bond (2.0). This result suggests that there may exist considerable conjugation over these rings. In addition, the stabilization energies $E(2)$ were calculated by means of the second-order perturbation theory. In the NBO analysis, $E(2)$ is used to describe the delocalization trend of electrons from the donor bond to the acceptor bond. The selected $E(2)$ for tri-*s*-triazine and its three nitrogen isoelectronic equivalents at the MP2/6-31G(d) level are summarized in Table 2, where BD and BD* denote bonding and antibonding natural bond orbitals and LP denotes the lone pair. Furthermore, these interactions are visualized: As shown in Table 2 and Figure 2, there exist strong donor−acceptor interactions among these tricyclic systems. The $E(2)$ values between the π bonding orbitals and π^* antibonding orbitals in the peripheries of these systems are in the range of 192−418 kJ mol^{-1}. The $E(2)$ interaction between the lone pair of the central nitrogen atom and the peripheral π^* antibonding orbitals is about 314 kJ mol^{-1}. This strong interaction implies that the central nitrogen participates in the conjugation and makes the three central N−C bonds shorter than a normal N−C single bond. Moreover, molecular orbital analysis shows there exist occupied delocalized π orbitals in tri-*s*-triazine and its three nitrogen isoelectronic equivalents. These orbitals are composed purely of $2p_z$ orbitals of all carbon and nitrogen atoms, and their stereographs are shown in Figure 3.

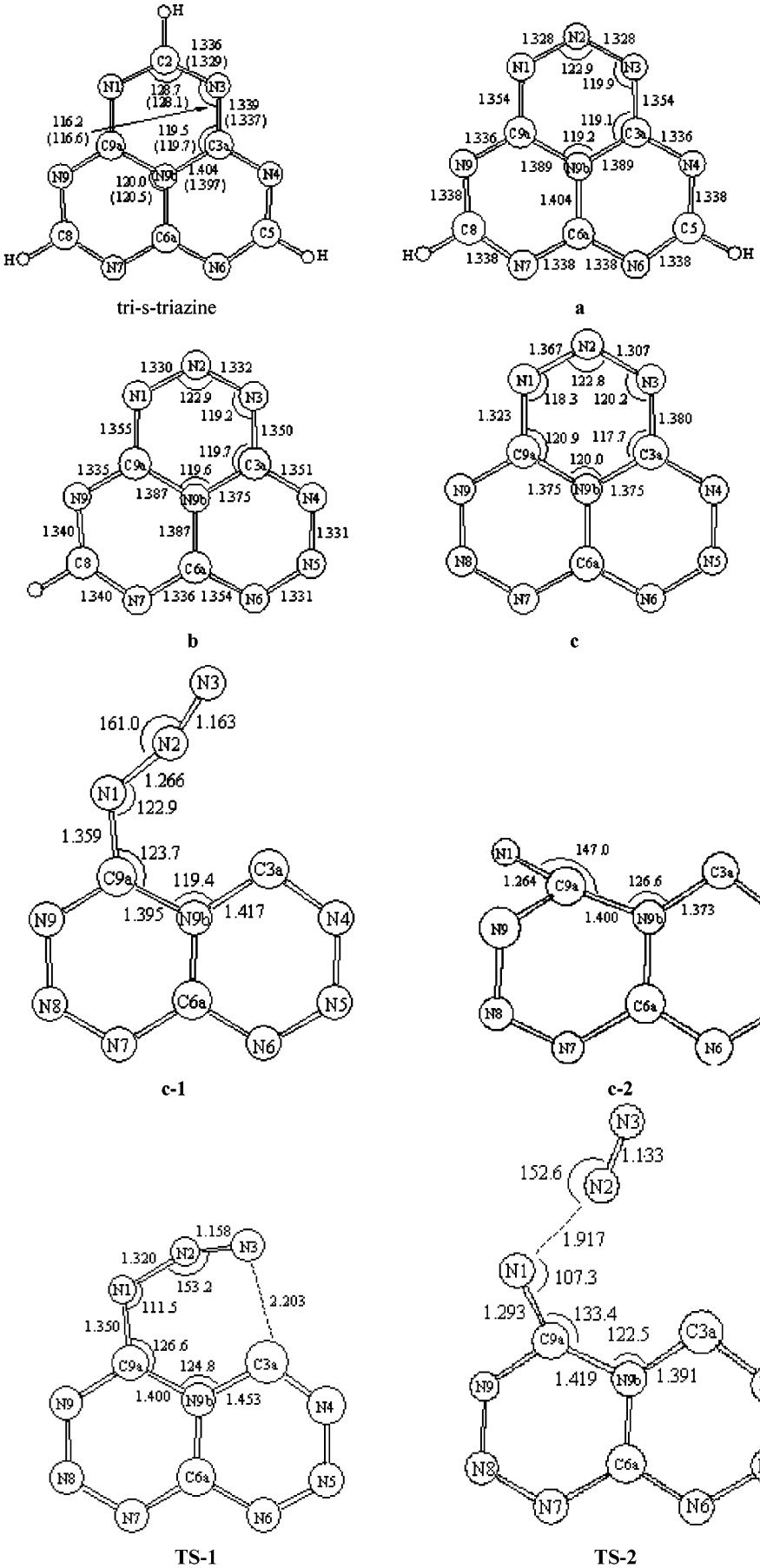

Figure 1. Optimized structures of tri-*s*-triazine and its nitrogen isoelectronic equivalents along with the main geometric parameters. Numbers in parentheses are the experimental values. Bond lengths are in angstroms and bond angles in degrees.

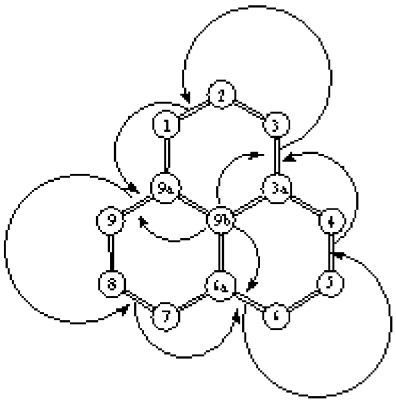

Figure 2. Interaction between π bonding orbitals and π^* antibonding orbitals and between the lone pair and π^* antibonding orbitals in tri-*s*-triazine and its nitrogen isoelectronic equivalents.

TABLE 2: Selected Stabilization Energies $E(2)$ (kJ mol^{-1}) for Tri-*s*-triazine and Its Nitrogen Isoelectronic Equivalents

	donor NBO	acceptor NBO	$E(2)$
tri-*s*-triazine	BD N1−C9a	BD* C2−N3	395.51
	BD C2−N3	BD* C3a−N4	363.28
	BD C3a−N4	BD* C5−N6	395.51
	BD C5−N6	BD* C6a−N7	363.28
	BD C6a−N7	BD* C8−N9	395.51
	BD C8−N9	BD* N1−C9a	363.28
	LP(1) N9b	BD* N4−C3a	311.08
	LP(1) N9b	BD* N7−C6a	311.08
	LP(1) N9b	BD* N1−C9a	311.08
a	BD N1−C9a	BD* N2−N3	423.64
	BD N2−N3	BD* C3a−N4	280.27
	BD C3a−N4	BD* C5−N6	379.63
	BD C5−N6	BD* C6a−N7	366.88
	BD C6a−N7	BD* C8−N9	390.54
	BD C8−N9	BD* N1−C9a	374.49
	LP(1) N9b	BD* N1−C9a	324.87
	LP(1) N9b	BD* C3a−N4	326.92
	LP(1) N9b	BD* C6a−N7	300.96
b	BD N1−N2	BD* N9−C9a	279.06
	BD N9−C9a	BD* N7−C8	373.15
	BD N7−C8	BD* N6−C6a	377.41
	BD N6−C6a	BD* N4−N5	417.58
	BD N4−N5	BD* N3−C3a	287.25
	BD N3−C3a	BD* N1−N2	400.53
	LP(1) N9b	BD* N3−C3a	335.82
	LP(1) N9b	BD* N6−C6a	315.00
	LP(1) N9b	BD* N9−C9a	317.14
c	BD N1−N2	BD* N9−C9a	192.91
	BD N9−C9a	BD* N7−N8	250.05
	BD N7−N8	BD* N6−C6a	192.91
	BD N6−C6a	BD* N4−N5	250.05
	BD N4−N5	BD* N3−C3a	192.91
	BD N3−C3a	BD* N1−N2	250.05
	LP(1) N9b	BD* N3−C3a	297.07
	LP(1) N9b	BD* N6−C6a	297.07
	LP(1) N9b	BD* N9−C9a	297.07

As discussed above, we find the tri-*s*-triazine and its three nitrogen isoelectronic equivalents all contain a large conjugation system, which is advantageous to their stabilities.

3. Electronic Topology. The $\rho(r)$ contour maps in the ring plane of the four molecules at MP2/6-31G(d)-optimized geometries are shown in Figure 4, where the locations of all the BCPs as well as the two RCPs are also displayed. This figure illustrates the power of the electron density as a tool to characterize molecular shape. These $\rho(r)$ contour maps of the four molecules are very similar. Coming from the largest values of $\rho(r)$ near the nuclei, there is a density contour of 0.4 au, which defines the outer domain of carbon and nitrogen atoms as an entity. This contour traces out a region around the nitrogen atoms with lone electron pairs larger than that around the carbons. An important change then occurs at the next plotted contour of 0.2 au, which encompasses the whole molecular body by a single isodensity contour that also defines the limit of the three rings. As well-known for organic molecules, this 0.2 au contour is usually used to define the connectivity while the outermost 0.001 au contour is known to an estimation of the van der Waals volume and is useful in molecular recognition and similar studies.[34]

The electronic density ρ_b and its Laplacian $\nabla^2\rho_b$ of the BCP are listed in Table 3. It has been shown that ρ_b and $\nabla^2\rho_b$ taken together can be employed to monitor the relative increase or decrease of charge accumulation. For all the species, C−N bonds on the periphery of the ring are different from those at the center: the electron density ρ_b is about 20% higher in the former case, and the corresponding Laplacian $\nabla^2\rho_b$ is significantly (about 60%) higher (more negative). We expect the local concentration of charge in the former case to be much higher. Comparing the N−N bonds and the C−N bonds on the periphery, it is clear that the former has a slightly higher electron density ρ_b (about 10%), but a remarkably (about 40%) lower (less negative) Laplacian $\nabla^2\rho_b$. This means that the local charge accumulation in the former is lower than that in the latter. Our attention is now turned to another parameter, ϵ, from AIM analysis. The ellipticity ϵ provides a measure of not only the π character of a bond but also its structural stability. Substantial bond ellipticities reflect structural instability; that is, the bond can easily be ruptured. In Table 3, we can see that ϵ for those peripheral C−N bonds connected with a central C−N bond is about 0.15, for the other peripheral C−N bonds it is about 0.03, for the central C−N bonds it is about 0.05, and for the N−N bonds it is about 0.10, confirming that the successive replacement of the CH groups by nitrogen atoms in tri-*s*-triazine will result in the successive decrease of the structural stability of the species.

The MEP plots for tri-*s*-triazine and its nitrogen isoelectronic equivalents (Figure 5) show that the positive electrostatic potential (shown in red) corresponds to the central region of the ring and the CH bonds, while the negative potential (shown in blue) is mainly associated with the peripheral nitrogen atoms. Moreover, along with the successive replacement of the CH groups by nitrogen atoms, the positive potential is strengthened and its region at the center of the ring is enlarged also. This result suggests that these heterocyclic rings should be applicable as an anion recognition module in cyclophane chemistry.

4. Heats of Formation and Relative Specific Impulse. Table 4 lists the total energies at 0 K (E_0) and enthalpies at 298 K (H_{298}) for the tri-*s*-triazine and its nitrogen isoelectronic equivalents calculated at the G3(MP2) level. To obtain the heat of formation $\Delta_f H_0$ values, the E_0 values of the constituent atoms were also required. At the G3(MP2) level, the E_0 values for C, H, and N are −37.78934, −0.50184, and −54.52519 hartrees. In the same way, the H_{298} values for the constituent atoms were also required in the calculation of $\Delta_f H_{298}$ values, and these quantities can be obtained by adding $E_{trans} + PV$ (= $2.5RT$ = 0.00236 hartrees at 298 K) to the atomic E_0 values.

Examining the values listed in the table, it is seen that the replacement of the CH groups by nitrogen atoms in the tri-*s*-triazine molecule will result in a substantial increase of the heats of formation for the products. As a consequence, the isoelectronic equivalent **c**, in which all the CH groups are replaced by the nitrogen atoms, has the highest heat of formation, $\Delta_f H_{298}$ = 1311.4 kJ mol^{-1}, while $\Delta_f H_{298}$ for tri-*s*-triazine is only 530.3 kJ mol^{-1}.

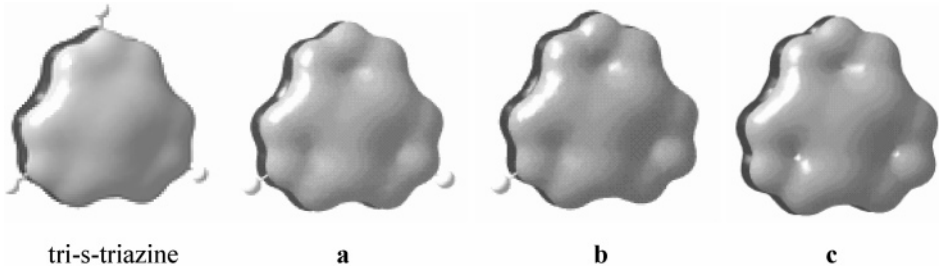

Figure 3. Delocalized π occupied orbitals in tri-*s*-triazine and its nitrogen isoelectronic equivalents.

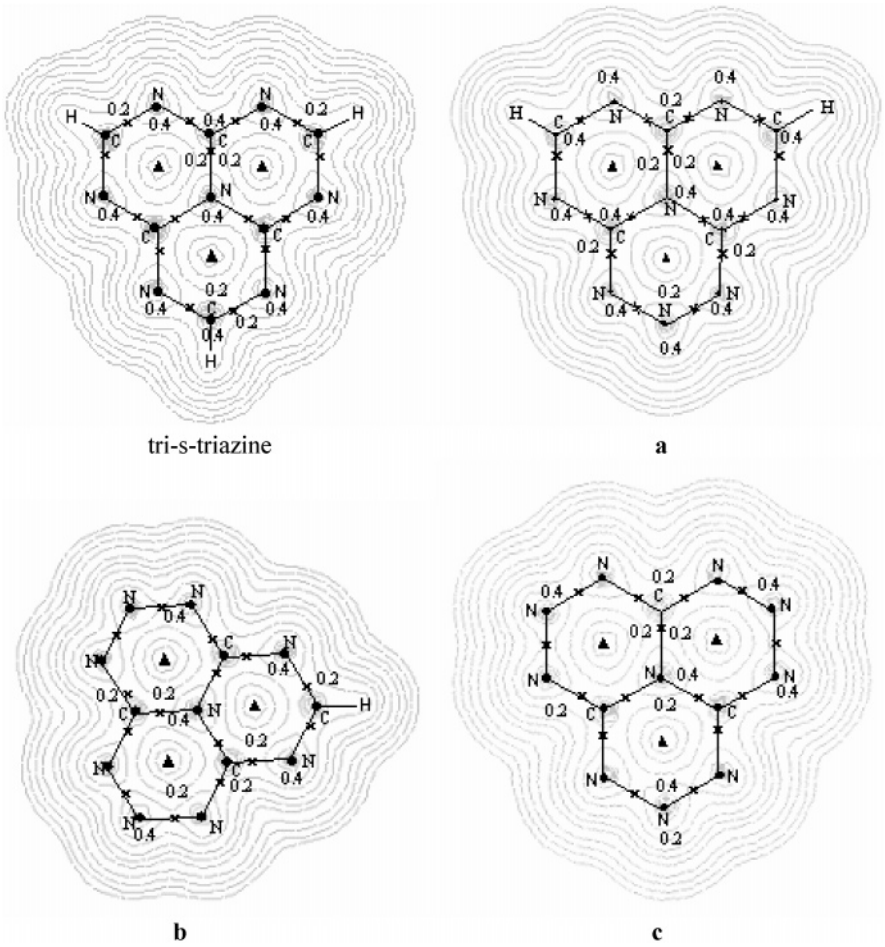

Figure 4. Contour map of the MP2/6-31G(d) electron density $\rho(r)$ in the molecular plane of tri-*s*-triazine and its nitrogen isoelectronic equivalents. Full circles indicate the location of nuclei, x's indicate BCPs, and triangles indicate RCPs.

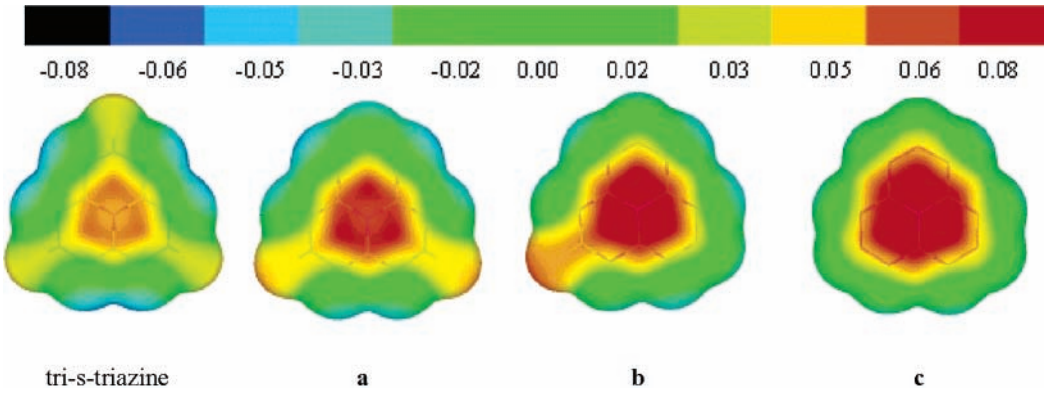

Figure 5. Calculated MP2/6-31G(d) electrostatic potential surfaces for tri-s-triazine and its nitrogen isoelectronic equivalents.

A previous study has shown that the nitrogen-rich compounds form a unique class of energetic materials deriving most of their very high positive heats of formation.[35,36] It is logical to envision some of the molecules studied here as potential candidates for HEDMs because of their rather high heats of formation. We calculated the specific impulses to evaluate the performance of

TABLE 3: Local Values (au) of the Electron Density ρ_b, Laplacian of the Electron Density $\nabla^2\rho_b$, and Ellipticity ϵ of the Bond Critical Points for Tri-s-triazine and Its Nitrogen Isoelectronic Equivalents

	tri-*s*-triazine			a			b			c		
	ρ_b	$\nabla^2\rho_b$	e	ρ_b	$\nabla^2\rho_b$	e	ρ_b	$\nabla^2\rho_b$	e	ρ_b	$\nabla^2\rho_b$	e
$N_1-C_2(N_2)$	0.3577	−1.1564	0.03	0.3998	−0.9572	0.10	0.3984	−0.9488	0.10	0.4185	−1.0132	0.14
$C_2(N_2)-N_3$	0.3577	−1.1564	0.03	0.3998	−0.5972	0.10	0.3972	−0.9484	0.10	0.3685	−0.8520	0.05
$N_4-C_5(N_5)$	0.3577	−1.1564	0.03	0.3556	−1.1492	0.03	0.3979	−0.9508	0.10	0.4185	−1.0132	0.14
$C_5(N_5)-N_6$	0.3577	−1.1564	0.03	0.3561	−1.1520	0.03	0.3976	−0.9464	0.10	0.3685	−0.8520	0.05
$N_7-C_8(N_8)$	0.3577	−1.1564	0.03	0.3561	−1.1524	0.03	0.3544	−1.1444	0.03	0.4185	−1.0132	0.14
$C_8(N_8)-N_9$	0.3577	−1.1564	0.03	0.3557	−1.1488	0.03	0.3540	−1.1472	0.03	0.3685	−0.8520	0.05
N_1-C_{9a}	0.3693	−1.5452	0.14	0.3637	−1.4788	0.15	0.3632	−1.4688	0.15	0.3468	−1.3208	0.10
N_3-C_{3a}	0.3693	−1.5452	0.14	0.3636	−1.4780	0.15	0.3662	−1.4812	0.16	0.3820	−1.5648	0.22
N_9-C_{9a}	0.3693	−1.5452	0.14	0.3712	−1.5444	0.14	0.3719	−1.5460	0.15	0.3820	−1.5648	0.22
N_4-C_{3a}	0.3693	−1.5452	0.14	0.3713	−1.5448	0.14	0.3657	−1.4760	0.16	0.3468	−1.3208	0.10
N_6-C_{6a}	0.3693	−1.5452	0.14	0.3698	−1.5456	0.14	0.3637	−1.4740	0.15	0.3820	−1.5648	0.22
N_7-C_{6a}	0.3693	−1.5452	0.14	0.3698	−1.5456	0.14	0.3715	−1.5432	0.15	0.3468	−1.3208	0.10
$C_{3a}-N_{9b}$	0.2960	−0.6748	0.05	0.3043	−0.6084	0.05	0.3110	−0.5420	0.05	0.3100	−0.5132	0.04
$C_{6a}-N_{9b}$	0.2960	−0.6748	0.05	0.2946	−0.6240	0.05	0.3032	−0.5572	0.05	0.3100	−0.5132	0.04
$C_{9a}-N_{9b}$	0.2960	−0.6748	0.05	0.3043	−0.6084	0.05	0.3033	−0.5572	0.05	0.3100	−0.5132	0.04

TABLE 4: Total Energies (hartrees) at 0 K (E_0), Enthalpies at 298 K (H_{298}), and Heats of Formation (kJ mol^{-1}) at 0 K ($\Delta_f H_0$) and 298 K ($\Delta_f H_{298}$) for Tri-s-triazine and Its Nitrogen Isoelectronic Equivalents Calculated with the G3(MP2) Method

	E_0	H_{298}	$\Delta_f H_0$	$\Delta_f H_{298}$
tri-*s*-triazine	−612.8343	−612.8254	553.7	530.3
a	−628.7977	−628.7888	807.8	785.0
b	−644.7595	−644.7508	1066.2	1043.3
c	−660.7177	−660.7091	1333.9	1311.4

TABLE 5: Idealized Stoichiometric Decomposition Reactions, Relative $\Delta_f H$, and Relative Specific Impulse I_s of HMX and Tri-s-triazine and Its Nitrogen Isoelectronic Equivalents

molecule	idealized stoichiometric reaction	relative $\Delta_f H$	I_s
HMX	$C_4N_8O_8H_8 \rightarrow 4CO + 4N_2 + 4H_2O$	1	1
tri-*s*-triazine	$C_6N_7H_3 \rightarrow {}^7/_2N_2 + {}^3/_2H_2 + 6C$	0.89	0.61
a	$C_5N_8H_2 \rightarrow 4N_2 + H_2 + 5C$	1.32	0.74
b	$C_4N_9H \rightarrow {}^9/_2N_2 + {}^1/_2H_2 + 4C$	1.75	0.86
c	$C_3N_{10} \rightarrow 5N_2 + 3C$	2.20	0.98

these species as HEDMs. To facilitate comparisons, our values are given relative to that of HMX (1,3,5,7-tetranitro-1,3,5,7-tetraazacyclooctane), a widely used HEDM. Our results in Table 5 show that the specific impulses of the isoelectronic equivalents increase substantially along with the replacement of the CH groups by nitrogen atoms. We can predict that equivalent **c** may be a good candidate for HEDM due to its high heat of formation and relative specific impulse.

5. Dissociation of Equivalent c. As discussed above, the equivalent **c**, C_3N_{10}, was identified as a good candidate for HEDM. To gain insight into its properties, we studied its dissociation mechanism in detail. First, we studied the dissociation of C_3N_{10} starting from one of the hexagons. The results in Figure 1 show that an azido group in **c-1** can be obtained from the rupture in one of the peripheral C−N bonds (N3−C3a). The major changes upon hexagonal ring opening are shown in the widening of the N1−N2−N3 angle to 40°, the shrinking of the N1−N2 and N2−N3 bonds by 0.10 and 0.14 Å, respectively, and the increase of the N1−C9a bond by 0.04 Å. The changes in the other two unruptured hexagons are negligible and are only seen in the angle and bonds related to three atoms, C3a, C9a, and N9b: the C3a−N9b and C9a−N9b bonds increase by about 0.02 and 0.04 Å, respectively, while the angle C3a−N9b−C9a remains almost unchanged. For the transition state **TS-1**, the N3····C3a distance increases from 1.35 to 2.203 Å, the N1−N2 bond falls between those in **c** and **c-1**, the C3a−N9b and C9a−N9b bonds are even slightly lengthened from those in **c-1**, and the N2−N3 bond is longer than those in **c** and **c-1**. As expected, the angle N1−N2−N3 in the transition state **TS-1** is between those of **c** and **c-1**. Table 6 shows the variations of energies in the decomposition of C_3N_{10} starting from the rupture in one of the hexagons. The decomposition reaction is calculated to be endothermic by 123.3 kJ mol^{-1} and possesses a fairly large activation barrier of 216.4 kJ mol^{-1} and a low reaction rate of 3.93×10^{-24} s^{-1}.

TABLE 6: Total Energy E (au), Formation Energy ΔE (kJ mol^{-1}), Activation Energy $\Delta E^{\ddagger}$ (kJ mol^{-1}), Relative Free Energy ΔG (kJ mol^{-1}), Reaction Rates k (s^{-1}), and the Two Lowest Frequencies (cm^{-1}) for the Intermediates and Transition States for the Decomposition of Equivalent c

	E (au)	ΔE	$\Delta E^{\ddagger}$	ΔG	K(298 K)	ν_1	ν_2
c	−659.7762					113.4	113.5
c-1	−659.7292	123.27				5.4	81.6
c-2	−550.4323	109.10				77.4	136.1
TS-1	−659.6937		216.40	206.41	3.93×10^{-24}	−543.6	60.0
TS-2	−659.6518		203.02	191.74	1.47×10^{-21}	−524.9	39.5

In the next step, we studied the decomposition of the azido group. As shown in Figure 1, the decomposition of the azido group in **c-1** yields **c-2** and N_2. In comparison with **c-1**, the detachment of a N_2 molecule results in increases of angles N1−C9a−N9b and C3a−N9b−C9a in **c-2** by about 25° and 7°, respectively, while the N1−C9a bond length decreases by 0.095 Å. The changes in the other bond lengths and bond angles are negligible. For the transition state **TS-2**, the N1····N2 distance increases to 1.917 Å, and the angle N1−C9a−N9b increases to 133.4°, which is larger than that in **c-1** but less than that in **c-2**. As shown in Table 6, the detachment of N_2 is endothermic by 109.1 kJ mol^{-1} and possesses a large activation barrier of 203.02 kJ mol^{-1} and a low reaction rate of 1.47×10^{-21} s^{-1}.

Conclusions

Ab initio quantum chemical calculations at the MP2/6-31G-(d) and G3(MP2) levels are reported on tri-*s*-triazine and its nitrogen isoelectronic equivalents. The geometric structures, electronic topologies, heats of formation, and relative specific impulses of these species and decomposition of C_3N_{10} are discussed in detail. The results reveal that these heterocyclic rings should be applicable as an anion recognition module in cyclophane chemistry, and among the equivalents studied, **c** is a potential HEDM.

Acknowledgment. This work was supported by the Research Grants Council of Hong Kong (Project Nos. 9040979 (CityU 102404) and CUHK4275/00P), Special Research Foundation

of Doctoral Education of the Chinese University (Grant 20020610024), and National Science Foundation of China (Grant 20373045).

References and Notes

(1) Korkin, A. A.; Bartlett, R. J. *J. Am. Chem. Soc.* **1996**, *118*, 12244.

(2) (a) Finkel'shtein, A. I. *Opt. Spektrosk.* **1959**, *6*, 33. (b) Morokuma, K.; Yonezawa, T.; Fukui, K. *Bull. Chem. Soc. Jpn.* **1962**, *35*, 1646. (c) Saigusa, H.; Lim, E. C. *J. Chem. Phys.* **1983**, *78*, 91. (d) Goates, S. R.; Chu, J. O.; Flynn, G. W. *J. Chem. Phys.* **1984**, *81*, 4521. (e) Zaruba, M.; Hilt, D.; Tennekoon, G. S. *Biochem. Biophys. Res. Commun.* **1985**, *129*, 522. (f) Korkin, A. A.; Bartlett, R. J. *J. Am. Chem. Soc.* **1996**, *118*, 12244. (g) Stringfield, T. W.; Shepherd, R. E. *Inorg. Chim. Acta* **1999**, *292*, 225.

(3) Zhan, Z.; Müllner, M.; Lercher, J. A. *Catal. Today* **1996**, *27*, 167.

(4) Liebig, J. *Ann. Pharm.* **1834**, *10*, 10.

(5) Gmelin, L. *Ann. Pharm.* **1835**, *15*, 252.

(6) Pauling, L.; Sturdivant, J. H. *Proc. Natl. Acad. Sci. U.S.A.* **1937**, *23*, 615.

(7) Wilson, E. K. *Chem. Eng. News* **2000**, *78* (32), 62.

(8) Rossman, M. A.; Leonard, N. J.; Urano, S.; LeBreton, P. R. *J. Am. Chem. Soc.* **1985**, *107*, 3884.

(9) Hosmane, R. S.; Rossman, M. A.; Leonard, N. J. *J. Am. Chem. Soc.* **1982**, *104*, 5497.

(10) Shahbaz, M.; Urano, S.; LeBreton, P. R.; Rossman, M. A.; Hosmane R. S.; Leonard, N. J. *J. Am. Chem. Soc.* **1984**, *106*, 2805.

(11) Shahbaz, M.; Urano, S.; LeBreton, P. R.; Rossman, M. A.; Hosmane R. S.; Leonard, N. J. *J. Am. Chem. Soc.* **1984**, *106*, 2805.

(12) Kroke, E.; Schwarz, M.; Bordon, E. H.; Kroll, P.; Noll, B.; Norman, A. D. *New J. Chem.* **2002**, *26*, 508.

(13) Jürgens, B.; Irran, E.; Senker, J.; Kroll, P.; Müller, H.; Schnick, W. *J. Am. Chem. Soc.* **2003**, *125*, 10288.

(14) Miller, D. R.; Swenson, D. C.; Gillan, E. G. *J. Am. Chem. Soc.* **2004**, *126*, 5372.

(15) (a) Redemann, C. E.; Lucas, H. J. *J. Am. Chem. Soc.* **1940**, *62*, 842. (b) Schroeder, H.; Kober, E. *J. Org. Chem.* **1962**, *27*, 4262. (c) Schroeder, H. (Olin Mathieson Chemical Corp., Virginia). U.S. Pat. US 3089875, 1963. (d) Finkelshtein, A. I.; Spiridonova, N. V. *Russ. Chem. Rev.* **1964**, *33*, 400. (e) Neef, R. (Bayer AG, Leverkusen, Germany). Ger. Pat. DE 1102321, 1961. (f) Gremmelmaier, C.; Riethmann, J. (Ciba-Geigy, New York). U.S. Pat. US 4205167 A, 1980.

(16) Zheng, W. X.; Wong, N. B.; Wang, W. Z.; Zhou, G.; Tian, A. M. *J. Phys. Chem. A* **2004**, *108*, 97.

(17) Carpenter, J. E.; Weinhold, F. *J. Mol. Struct.*: *THEOCHEM* **1988**, *169*, 41.

(18) Reed, A. E.; Curtiss, L. A.; Weinhold, F. *Chem. Rev.* **1988**, *88*, 899.

(19) Foster, J. P.; Weinhold, F. *J. Am. Chem. Soc.* **1980**, *102*, 7211.

(20) Reed, A. E.; Weinstock, R. B.; Weinhold, F. J. *Chem. Phys.* **1985**, *83*, 735.

(21) Frisch, M. J.; Trucks, G. W.; Schlegel, H. B.; Scuseria, G. E.; Robb, M. A.; Cheeseman, J. R.; Zakrzewski, V. G.; Montgomery, J. A., Jr.; Stratmann, R. E.; Burant, J. C.; Dapprich, S.; Millam, J. M.; Daniels, A. D.; Kudin, K. N.; Strain, M. C.; Farkas, O.; Tomasi, J.; Barone, V.; Cossi, M.; Cammi, R.; Mennucci, B.; Pomelli, C.; Adamo, C.; Clifford, S.; Ochterski, J.; Petersson, G. A.; Ayala, P. Y.; Cui, Q.; Morokuma, K.; Malick, D. K.; Rabuck, A. D.; Raghavachari, K.; Foresman, J. B.; Cioslowski, J.; Ortiz, J. V.; Stefanov, B. B.; Liu, G.; Liashenko, A.; Piskorz, P.; Komaromi, I.; Gomperts, R.; Martin, R. L.; Fox, D. J.; Keith, T.; Al-Laham, M. A.; Peng, C. Y.; Nanayakkara, A.; Gonzalez, C.; Challacombe, M.; Gill, P. M. W.; Johnson, B. G.; Chen, W.; Wong, M. W.; Andres, J. L.; Head-Gordon, M.; Replogle, E. S.; Pople, J. A. *Gaussian 98*, revision A.11; Gaussian, Inc.: Pittsburgh, PA, 1998.

(22) Bader, R. F. W. *Atoms in Molecules, A Quantum Theory*; International Series of Monographs in Chemistry; Oxford University Press: Oxford, 1990; Vol. 22.

(23) Biegler-König, F.; Schönbohm, J.; Derdau, R.; Bayles, D.; Bader, R. F. W. *AIM 2000*, Version 2.0; McMaster University: Hamilton, Ontario, Canada, 2002.

(24) Politzer, P.; Murray, J. S. In *Molecular Electrostatic Potentials*: *Concepts and Applications*; Murray, J. S., Sen, K. D., Eds.; Elsevier: Amsterdam, 1996; p 649.

(25) Boris, B.; Petia, B. *J. Phys. Chem. A* **1999**, *103*, 6793.

(26) Gadre, S. R.; Bhadane, P. K. *J. Phys. Chem. A* **1999**, *103*, 3512.

(27) Laaksonen, L. *J. Mol. Graphics* **1992**, *10*, 33.

(28) Bergman, D. L.; Laaksonen, L.; Laaksonen, A. *J. Mol. Graphics Modell.* **1997**, *15*, 301.

(29) Curtiss, L. A.; Redfern, P. C.; Raghavachari, K.; Rassolov, V.; Pople, J. A. *J. Chem. Phys*. **1999**, *110*, 4703.

(30) Nicolaides, A.; Radom, L. *Mol. Phys*. **1996**, *88*, 759.

(31) Lias, S. G.; Bartmess, J. E.; Liebman, J. F.; Holmes, J. L.; Levin, R. D.; Mallard, W. G. *Journal of Physical and Chemical Reference Data*; American Institute of Physics, Inc.: New York, 1988; Suppl. 1.

(32) Politzer, P.; Murray, J. S.; Grice, M. E.; Sjoberg, P. In *Chemistry of Energetic Materials*; Olah, G. A., Squire, D. R., Eds.; Academic Press: San Diego, CA, 1991; pp 77−93.

(33) Hosmane, R. S.; Rossman, M. A.; Leonard, N. J. *J. Am. Chem. Soc.* **1982**, *104*, 5497.

(34) Mezey, P. G. *Shape in Chemistry. An Introduction to Molecular Shape and Topology*; VCH: New York, 1993.

(35) Zhang, M. X.; Eaton, P. E.; Gilardi, R. D. *Angew. Chem.* **2000**, *112*, 422.

(36) Zhang, M. X.; Eaton, P. E.; Gilardi, R. D. *Angew. Chem., Int. Ed.* **2000**, *39*, 401.